Stratification in Bidisperse Polymer Brushes from Neutron Reflectivity

Rastislav Levicky,[†] Nagraj Koneripalli,[‡] and Matthew Tirrell*

Department of Chemical Engineering and Materials Science, University of Minnesota, Minneapolis, Minnesota 55455

Sushil K. Satija

NIST Center for Neutron Research, National Institute of Standards and Technology, Gaithersburg, Maryland, 20899

Received August 25, 1997; Revised Manuscript Received January 15, 1998

ABSTRACT: Two-component (bidisperse) polystyrene brushes, consisting of long and short chain populations end-tethered at a solid/liquid interface, were studied in toluene and cyclohexane solvents using neutron reflection methods. A stratification of the long and short chain components was observed under all solvent conditions, with a maximum in the long chain volume fraction profile occurring at the outer edge of the brush. The short chains resided in the inner brush region nearer to the substrate. Comparison of experimentally derived volume fraction profiles to analytical self-consistent mean-field theory predictions revealed qualitative agreement; however, the experimentally observed stratification is less pronounced. Furthermore, under the poorer, near-Θ conditions in cyclohexane, the total volume fraction profile was rather featureless and did not exhibit the characteristic bidisperse shape present in toluene.

Introduction

Polymer brushes, consisting of a set of polymer chains tethered by one end to a surface, offer a general framework for the description of many polymer systems in which chains are attached into a larger structure.[1] The mutual proximity of the chains in a polymer brush and the requirement of self-avoidance causes them to stretch away from the tethering surface. The early scaling theory analyses[2] of Alexander and deGennes revealed that the chain stretching can be viewed as arising from a balance between two dominant contributions: repulsive segment/segment interactions that favor dilution of segmental density and a swelling of the brush and an opposing elastic contribution that grows more pronounced with brush swelling and reflects the resistance of the chains to being deformed from their preferred coiled state.

While neutron scattering methods have provided extensive information on the structure of single component polymer brushes in a variety of solvent environments,[3−7] only limited experimental data[8] exist regarding the structure of bidisperse brushes comprised of two chain populations with different molecular weights. Bidisperse brushes arguably provide one of the simplest examples of a multicomponent end-tethered structure and thus present an appropriate starting place to investigate how the organization of such systems might be tailored. Theoretical[9−11] as well as simulation studies[12,13] have demonstrated that a bidisperse brush can be viewed as consisting of "inner" and "outer" regions. The outer brush region primarily contains longer chain portions "squeezed out" to the brush periphery in order to relieve the crowding in the inner brush where the short chains must reside. This chain-length-sensitive stratification gives rise to a maximum in the long chain volume fraction profile near the outer brush edge. Furthermore, the ends of the longer chains are exiled to the brush periphery and excluded from the sterically crowded inner brush. In this sense, a synthetic bidisperse brush can achieve an effect similar to membrane proteins in biological cells, which make a receptor more accessible by placing it above the steric barrier of the membrane's carbohydrate corona.[14] As studies in the surface-forces apparatus have shown,[15,16] controlling brush composition can be also used to tune the interaction potential between brush-bearing surfaces. For example, such interfacial modification is relevant to applications in the stabilization of multiphasic systems[17] and lubrication.[18]

Despite the versatility of bidisperse brush properties, direct experimental evidence about their structure is scarce. In a recent neutron reflectivity study, Kent *et al.*[8] reported the overall density profile (sum of long and short chains) for brushes immersed in a good solvent. Several different molecular weight ratios of the two components and chain surface densities were employed. The brushes were constructed from Langmuir monolayers of diblock copolymers where the soluble polystyrene block of each chain was tethered to an ethyl benzoate/air interface by an insoluble poly(dimethylsiloxane) block. Surface density was controlled by compression of the monolayer by a movable barrier. Relative to pure monolayers with same surface density of long chains, excess stretching of up to ∼30% of the long chains was observed for a molecular weight ratio $N_L/N_S \approx 3$, where N_L and N_S are the number of monomers in the long and short chains, respectively. Additionally, total volume fraction profiles possessing distinct inner and outer brush regions separated by a "kink" in the profile were reported.[8]

While the study of Kent et al.[8] furnished interesting insights into the structure of bidisperse brushes, the individual long and short chain profiles were not

* To whom correspondence should be addressed.
[†] Presently at the National Institute of Standards and Technology, Bldg. 221/A303, Gaithersburg, Maryland 20899.
[‡] Presently at 3M Corporate Research Science Research Laboratory, 201−2N-19 3M Center, St. Paul, Minnesota 55144.

S0024-9297(97)01278-3 CCC: $15.00
Published on Web 03/31/1998

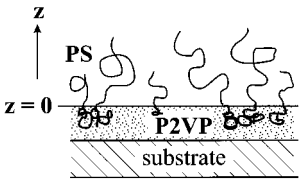

Figure 1. Schematic diagram of a bidisperse brush sample. Mixed films of P2VP−PS block copolymers were spin coated and annealed. After exposure to a PS selective solvent, the outer PS layer swelled to form a bidisperse brush while the P2VP layer served to anchor it to the substrate.

obtained and only good solvent conditions were addressed. The neutron reflectivity study presented here provides experimental evidence of the stratified brush architecture by separately determining the short and long chain distributions. Furthermore, the effects of solvent quality are studied by employing both good as well as poorer, near-Θ solvent conditions. We conclude by comparing the experimental volume fraction profiles to those predicted by analytical self-consistent mean-field (ASCMF) calculations.[9,10]

Experimental Methods

The polymers used were anionically synthesized, symmetric poly(styrene-*b*-2-vinylpyridine) (PS−P2VP) block copolymers that have been characterized by gel permeation chromatography and static light scattering.[19] The polydispersities of all the block copolymers were ∼1.12. Toluene solutions containing two block copolymers differing in molecular weight were spin coated to form bidisperse polymer films on 100 mm diameter, 13 mm thick polished silicon wafer substrates. Immediately prior to spin coating the substrates were cleaned in a 70% H_2SO_4/10% H_2O_2/20% H_2O solution at 120 °C for 15 min, rinsed with deionized water, and dried under high purity nitrogen stream. *WARNING! The cleaning solution is extremely oxidizing and must not be stored in tightly sealed containers.* The spin coated films were annealed under vacuum for 4 days at 185 °C to facilitate the segregation of the blocks into a bottom P2VP layer next to the substrate and an upper PS layer at the ambient interface. When placed under toluene or cyclohexane, the PS layer swelled and formed a bidisperse brush while the insoluble P2VP layer anchored the brush to the substrate (Figure 1). Continuous monolayers were easily manufactured because P2VP wets the native oxide of the silicon substrates. The amount of spin coated material was sufficiently low so that all polymer was incorporated into a single monolayer. The spin coating technique offers a convenient alternative to chemically attaching homopolymer chains to the substrate,[4,6] and results in brushes of comparably high surface densities.

The properties of the two samples examined in the present study are listed in Table 1. Both samples possessed the same long chain component with a 103K ($K = 10^3$ g/mol) perdeuterated polystyrene (dPS) block. The shorter chains were also similar in size: 59K for sample 1 and 52K for sample 2. We note that the mole fraction x_L of longer chains was higher in sample 1 ($x_L = 0.36$) than in sample 2 ($x_L = 0.23$). In addition, in sample 1 both the long and short PS blocks were perdeuterated—hence, no contrast between the two was present, and only the total volume fraction profile was measured. However, in sample 2 the short chains were unlabeled polystyrene (hPS) while the long chains were dPS; therefore, matching the neutron contrast of the solvent to that of hPS (dPS) enabled independent determination of the long (short) chain volume fraction profiles. Contrast matching was attained by mixing appropriate quantities of unlabeled and perdeuterated solvents. The neutron scattering length density (SLD) of hPS equals 1.41×10^{-6} Å^{-2}—to contrast match it in cyclohexane a 75.8%:24.2% C_6H_{12}:C_6D_{12} solution was required while for toluene a 90.0%:10.0% C_7H_8:C_7D_8 solution was needed.[20] To contrast match cyclohexane to dPS (SLD = 6.47 $\times 10^{-6}$ Å^{-2}) a 3.3%:96.7% C_6H_{12}:C_6D_{12} mixture was prepared. However, it is not possible to fully contrast match toluene to dPS since the highest SLD possible (pure C_7D_8) is 5.66×10^{-6} Å^{-2}. The best that can be done is to use pure C_7D_8. Since the reflectivity depends approximately on the square of the SLD gradient,[21] in C_7D_8 the signal from the hPS short chains is still enhanced by a factor of $\sim((5.66 - 1.41)/\Delta z)^2(6.47 - 5.66)/\Delta z)^{-2} \approx 28$ over that arising from the imperfectly contrast matched dPS.

Specular NR measurements were performed on the NG7 reflectometer at NIST using 4.77 Å neutrons up to a momentum transfer $q_z = 0.1$ Å^{-1} ($q_z = 4\pi(\sin\theta)/\lambda$, θ is the glancing angle of incidence and λ the neutron wavelength). A temperature-controlled solvent cell, details of which will be described elsewhere,[22] held the samples during measurement. Both samples were studied under three different solvent qualities: toluene at 31 °C, cyclohexane at 60 °C, and cyclohexane at 31 °C. The samples were checked for swelling equilibrium by repeating the first half of each reflectivity scan 2 h later. The two sets of data always superposed.

The data were analyzed by comparing experimental reflectivities with those calculated from trial sample structures.[21] The native, ∼10 Å thick silicon oxide layer was modeled by a box function. The anchoring P2VP layer was also represented by a box function, while the concentration profile in the PS brush was modeled by one or two successive functions of the form $SLD(z) = SLD1 + SLD2(1 - (z/H)^n)^m$ where SLD(z) is the sample scattering length density at z, $z = 0$ corresponds to the PS/P2VP interface (Figure 1), SLD1 = SLD(H), SLD1 + SLD2 = SLD(0), and H is the z-extent of the modeling function. The exponent m was fixed at unity and SLD1 was fixed at the solvent SLD, but SLD2, H, and n were varied to optimize the agreement between calculated and experimental reflectivities. The interfaces between all layers were smeared to the desired width by convoluting an adjustable width Gaussian with the SLD profile within three standard deviations on both sides of the interface (for an interface between two box functions this procedure yields an error function shape). The SLD profiles were then discretized into 3 Å wide slivers, and the recursive Parrat method[23] was applied to calculate the reflectivity. The finalized brush SLD profiles were converted to polymer volume fractions which were numerically integrated to verify conservation of polymer. For each of the samples, agreement was within ±5%, thus quantifying the internal consistency of the data analysis.

Results and Discussion

Volume Fraction Profiles. Figure 2A displays the reflectivity data (points) for sample 1, while Figure 2B shows the data for sample 2 when the long dPS chains were contrast-matched out by the solvent and only the short hPS chains were "visible". The complementary situation of visible long chains is plotted in Figure 2C. Data are shown for all three solvent conditions studied: toluene at 31 °C, cyclohexane at 60 °C, and cyclohexane at 31 °C. For clarity, the reflectivity curves have been vertically offset and most of the error bars have been omitted. The solid lines are the calculated reflectivity fits.

The brush volume fraction profiles corresponding to the fits in Figure 2 are displayed in Figure 3. In the case of sample 1 (Figure 3A), the volume fraction represents the total polymer concentration $\Phi(z)$ since there was no contrast between long and short chains. Parts B and C of Figure 3 show the respective short $\Phi(z)_S$ and long chain $\Phi(z)_L$ volume fraction profiles for sample 2. The vertical lines at $z = 0$ separate a ∼ 50 Å wide P2VP/PS interfacial region, throughout which the covalent junctions between the two blocks were distributed, from the main body of the brush.[24] Compared to the swollen width of the PS brush (Figure 3), the

Table 1. Sample Characteristics

sample	longer chain M_n ($K = 10^3$ g/mol)[a]	shorter chain M_n ($K = 10^3$ g/mol)[a]	x_L[b]	α[c]	σ_i (chains/Å^2)[d]	σ_0 (chains/Å^2)[e]
1	dPS_{103K}−$hP2VP_{113K}$	dPS_{59K}−$hP2VP_{65K}$	0.36	0.75	0.00093	0.00033
2	dPS_{103K}−$hP2VP_{113K}$	hPS_{52K}−$hP2VP_{58K}$	0.23	0.84	0.00068	0.00016

[a] The prefixes d and h refer to perdeuterated and unlabeled polymer, respectively. [b] The mole fraction x_L of the longer PS blocks in the brush was taken to equal the spin coating solution value for sample 1. For sample 2 it was calculated by integrating the dry state scattering length density profile of the PS domain. [c] The size asymmetry parameter $\alpha = (N_L - N_S)/N_S$ where N is the degree of polymerization.[d] The total surface density of chains σ_i was estimated from dry state thickness and composition (x_L) of the PS layers. [e] $\sigma_0 = x_L\sigma_i$ equals the surface density of the long chains.

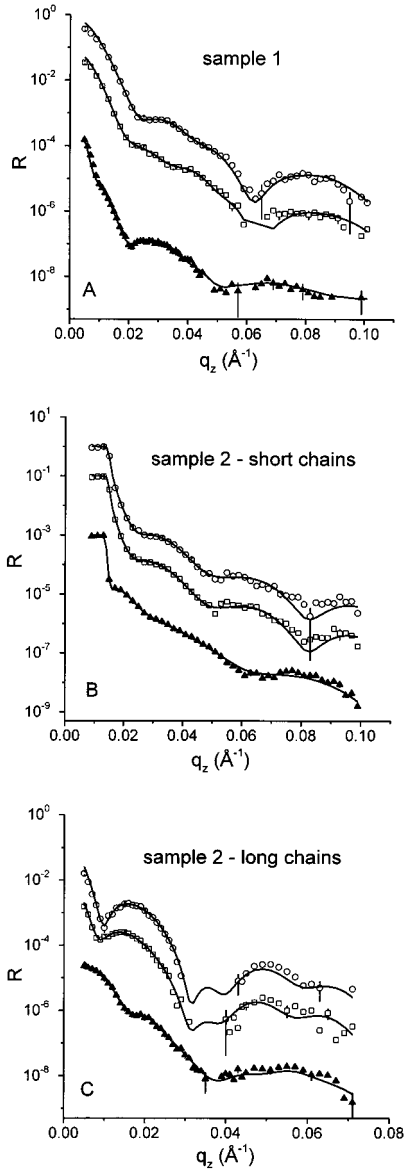

Figure 2. Reflectivity data for (A) sample 1, (B) sample 2 with just the short chains visible, and (C) sample 2 with the long chains visible. Experimental data: (○) cyclohexane at 31 °C, (□) cyclohexane at 60 °C shifted down by 1 order of magnitude, (▲) toluene at 31 °C shifted down by 3 orders of magnitude. Calculated fits are shown as the solid lines. The data have been vertically offset for clarity, and error bars are shown for every fifth point only. Data points not used in calculations due to low reflectivity signal are not displayed.

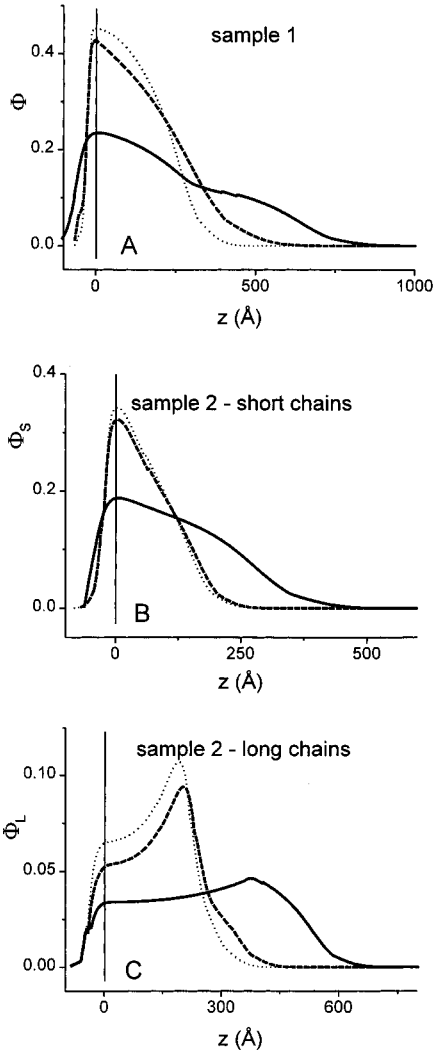

Figure 3. Volume fraction profiles for (A) sample 1, (B) sample 2 short chains, and (C) sample 2 long chains. Solvent: (—) toluene at 31 °C, (---) cyclohexane at 60 °C, (···) cyclohexane at 31 °C.

thickness of the P2VP anchoring layer did not vary significantly with solvent quality. For sample 1 the anchoring layer thickness was 130 Å under cyclohexane and 140 Å under toluene, while for sample 2 good fits were obtained with 125 Å under both cyclohexane and toluene.

Initial washing of sample 1 with cyclohexane resulted in a modest decrease in dry film thickness by 15 Å, with no additional loss observed during subsequent solvent exposures. The dry state widths of the P2VP (125 Å) and PS layers (103 Å) yielded a volume fraction of PS of 0.45, close to the nominal block copolymer composition of 0.48. For sample 2 the dry layer widths were 105 Å for PS and 135 Å for P2VP prior to the initial solvent exposure. However, during the initial solvent wash the film thickness decreased by 45 Å with 35 Å coming from a decrease in the PS domain dimension. The reason more PS than P2VP was eluted is likely 2-fold. First, gel permeation chromatographs indicate about a 5% content of a lower molecular weight component in the 110K hPS−hP2VP copolymer. This component can be

attributed to unreacted PS blocks from the synthesis, whose elution during the initial swelling of the film accounts for about a 10 Å decrease. Second, a preferential loosening and elution of copolymers with statistically larger PS blocks and smaller, more weakly anchored P2VP blocks is likely since it would decrease the steric repulsions present in the solvated brush. We emphasize that no additional loss of material was detected during subsequent exposures to solvent. In particular, for all measurements used to study the bidisperse brush structure, the amount of PS was within 70 ± 3 Å.

Under toluene, the brush experiences "good solvent" conditions characterized by positive values of the excluded volume parameter[25] $v \approx 0.3$, while in cyclohexane the system is close to the "Θ condition" where the excluded volume becomes zero. In the dilute limit, the Θ condition for PS in cyclohexane occurs between 30 and 40 °C depending on deuteration.[26] Thus passing from toluene to cyclohexane at 31 °C reveals the characteristics of brush structure in both good and near-Θ solvents. A simple model of the bidisperse brush is to consider it as consisting of two brushes: an inner brush characterized by a chain surface density $\sigma_i = \sigma_L + \sigma_S$ (the subscripts L and S refer to long and short chains respectively) and chain length N_S, and an outer brush (stacked on top of the inner brush) with a sparser surface density $\sigma_o = \sigma_L$ and chain length $(N_L - N_S)$.[27] The values of σ_i and σ_o have been calculated from the sample composition and dry state thickness and are listed in Table 1. These values indicate that the outer brush is three to four times less dense than the inner brush.

For sample 1, the total volume fraction profile in toluene exhibits an inflection at $z \approx 350$ Å (Figure 3A). The presence of an inflection under good solvent conditions agrees with previous theoretical observations[9−11] and simulations,[12,13] as well as experimental observations.[8] In toluene, the chains in both the inner and outer brushes are sufficiently stretched to produce distinct, brushlike profiles. However, in the poorer solvent cyclohexane at 60 °C and 31 °C volume fraction profiles without an inflection were obtained. Attempts to introduce a more distinct outer brush structure led to worsened fits to the experimental reflectivity. As discussed later, the lack of structure in the brush profiles arises from the poorer solvent conditions. In fact, in cyclohexane it is difficult to tell from the total volume fraction profiles that the brush is bidisperse.

The question then arises as to the actual degree of stratification present under the various solvent qualities. To answer this question we consider the short and long chain volume fraction profiles obtained for sample 2. From the $\Phi(z)_L$ profiles in Figure 3C, it is evident that the long chain volume fractions exhibit a maximum near the outer edge of the brush under all solvent qualities studied. In contrast, the short chain profiles decay monotonically with the greatest concentration occurring near $z = 0$ (Figure 3B). The presence of a maximum in $\Phi(z)_L$ provides direct evidence of the length-dependent stratification whereby the longer chains are segregated to the brush periphery. The stratification is clearly present under Θ as well as good solvent conditions. In addition, it can be deduced that the two chain lengths must be well mixed at the molecular level. If a lateral phase separation had occurred, $\Phi(z)_L$ should mimic a monodisperse brush with a monotonically decreasing parabolic-type profile[28] and hence would not exhibit a maximum.

The brush thickness for sample 1 decreased from ∼800 to ∼380 Å on passing from toluene to cyclohexane at 31 °C, whereas for sample 2 it decreased from ∼ 650 to ∼ 350 Å. The brush widths are greater for sample 1 because of higher chain surface densities as well as a higher mole fraction of the long chains (Table 1). While interesting predictions have been made regarding the interdependence of brush dimensions, brush composition x_L and size asymmetry $\alpha = (N_L - N_S)/N_S$,[9,10,13,27] a more extensive data set than presently available is necessary to test them. However, we can compare the shapes of the volume fraction profiles to those expected from analytical self-consistent mean-field (ASCMF) calculations.[9,10] This is done in the next section.

Comparison to ASCMF Predictions. The theoretical ASCMF expressions were taken from Birshtein et al.[10] who have reported an extensive analysis of the bidisperse brush (eqns 23−25, A1.17, A1.18, A1.23, and A1.24 of ref 10). We perform the comparison in scaled coordinates by dividing the vertical axis in Figures 3 by Φ(0) and the horizontal axis by the z-component rms dimension $R_{gz} = \langle z^2 \rangle - \langle z \rangle^2$, where $\langle z^2 \rangle$ and $\langle z \rangle$ are the second and first moments of the normalized total volume fraction profile, $\Phi(z)/\int \Phi(z)\, dz$. For sample 2, $\Phi(z)$ was obtained from $\Phi(z) = \Phi(z)_L + \Phi(z)_S$. Unlike in the theory, in the experiment the brush chains do not have their tethered ends localized at an ideally sharp planar surface; instead, these ends are distributed throughout the ∼50 Å wide interface between the P2VP anchoring layer and the brush body. Therefore, for purposes of overlaying the experimental data and the ASCMF profiles, we assumed the "tethering plane" to be in the center of the P2VP/brush interface. We emphasize that, in the scaled coordinates, there are no adjustable parameters in the ASCMF profiles as their shapes are completely determined by the values of x_L and α listed in Table 1. Since the qualitative features of the profiles in cyclohexane were quite similar at 31 and 60 °C, we do not present comparisons for the 60 °C data.

We compare the sample 1 $\Phi(z)$, as measured in toluene, to ASCMF predictions for good solvent conditions in Figure 4A. Comparison between the cyclohexane data and theta solvent ASCMF profiles is shown in Figure 4B. The experimental R_{gz} was 200 Å in toluene and 90 Å in cyclohexane at 31 °C. The toluene data and the theoretical good solvent prediction are observed to be in close agreement. Both profiles display a clear presence of inner and outer brush regions, and the widths of the profiles are quite similar. On the other hand, the 31 °C cyclohexane data in Figure 4B show noticeable deviations when compared to the ASCMF prediction for a Θ solvent. In particular, in contrast to the ASCMF profile, the experimental $\Phi(z)$ does not possess a clear outer brush region and decreases in a featureless manner to zero.

The total volume fraction profile $\Phi(z)$ for sample 2, as obtained in toluene, is compared to the ASCMF prediction for a good solvent in Figure 4C. The experimental $\Phi(z)$ profile was obtained from the sum of the short and long chain profiles $\Phi(z)_S$ and $\Phi(z)_L$, which are displayed in Figure 4E. An analogous comparison is carried out for the 31 °C cyclohexane data and ASCMF theta solvent predictions in parts D and F of Figure 4. The experimental R_{gz} values were 140 Å in toluene and 80 Å in 31 °C cyclohexane. In regard to the total volume

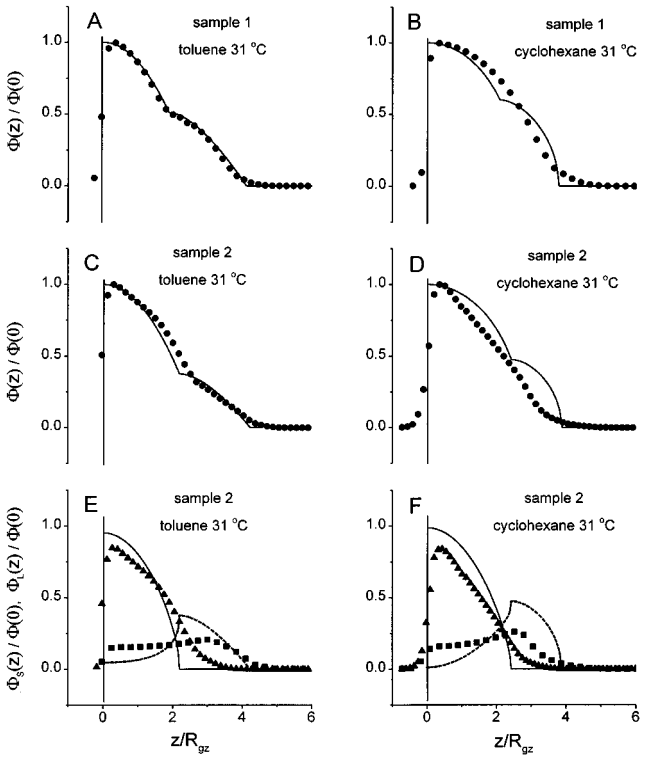

Figure 4. Comparison between experimental and analytical self-consistent mean-field[10] (ASCMF) volume fraction profiles. (A) and (B): sample 1 (●) experimental and (—) ASCMF total volume fraction profiles. (C) and (D): sample 2 (●) experimental and (—) ASCMF total volume fraction profiles. (E) and (F): sample 2 (▲) experimental short chain profile; (■) experimental long chain profile; (—) ASCMF short chain profile; (---) ASCMF long chain profile. In the ASCMF profiles $\Phi_L = \Phi$ in the outer brush since only the longer chains are present. The ASCMF expressions are given in ref 10. Please refer to the text for further discussion.

fraction profile $\Phi(z)$, similar comments hold as for the sample 1 data. In toluene, the experimental and theoretical $\Phi(z)$ profiles are quite similar. While there is a slight shift in the location of the inflection, we believe the shift is within our ability to specify α. As was also observed for sample 1, the experimental $\Phi(z)$ in cyclohexane does not exhibit a well-defined outer brush region. Both samples thus indicate good agreement between theoretical and experimental $\Phi(z)$ under good solvent conditions but poorer agreement near the Θ condition.

We can also compare the individual component profiles $\Phi(z)_S$ and $\Phi(z)_L$. As is evident from parts E and F of Figure 4, both experiment and theory indicate that the long and short chains are vertically stratified with a maximum in $\Phi(z)_L$ near the outer brush edge; therefore, the qualitative features of the theoretical predictions are borne out in the experiment. However, it is also evident that the experimental stratification is less dramatic than that predicted by the ASCMF theory. For example, $\Phi(z)_S/\Phi(0)$ is lower by $\sim$ 10% in the inner brush and extends $\sim$30% farther than the theoretical prediction. Additionally, $\Phi(z)_L/\Phi(0)$ is greater by a factor of $\sim$ 4 in the inner brush while in the outer brush it is only $\sim^1/_2$ of the predicted value. These differences occur under both solvent conditions. In particular, they are present in toluene despite the close agreement in the shape of the total volume fraction profile $\Phi(z)$.

In the ASCMF theory, it is always assumed that the brush chains are strongly stretched so that fluctuations of the chain around the lowest free energy configuration can be neglected.[9,10,28] The volume fraction profiles are calculated on the basis of this assumption. The accord with experimental $\Phi(z)$ under good solvent conditions, when the PS brush is most swollen, suggests that the chains are sufficiently stretched to fall within the regime where the theory is applicable. However, it is more difficult to see why the experimentally observed stratification is so much weaker than predicted from theory, especially in light of the good agreement in $\Phi(z)$. Some smearing of the experimental $\Phi(z)_S$ and $\Phi(z)_L$ profiles is expected because neither the long nor the short chains are strictly monodisperse, and the distribution of molecular lengths will lead to less sharply defined features. In addition, as mentioned earlier, not all brush chains are tethered at the same z position which may also smear out the profile features. However, Monte Carlo simulations[13] of bidisperse brushes of perfectly monodisperse chain populations tethered on strictly planar surfaces also indicate weaker stratification than obtained from ASCMF predictions. This leads us to conclude that, while relevant, the experimental factors mentioned above are not the sole source of the differences. In particular, approximations present in ASCMF theories such as working in the high molecular weight, strongly stretched limit[9,10,28] are also responsible. Numerical SCMF calculations,[11] in which the strong stretching assumption is relaxed and thermal fluctuations around the lowest energy configuration are allowed, exhibit weaker stratification what places them more in line with the present experimental observations. For example, in contrast to the ASCMF approach, the numerical calculations allow the shorter chains to partially penetrate into the outer brush.[11]

To estimate the effect of thermal fluctuations, we can consider the density correlation length ξ over which such fluctuations occur. For the stretched chains in a polymer brush, ξ is expected to be on the order of the lateral interchain separation.[2,4] Using the values of σ_i and σ_o for sample 2 (Table 1), we expect ξ to vary between $\sim$50 and $\sim$100 Å. This corresponds to $\sim 0.5R_{gz}$ to $1R_{gz}$ in parts E and F of Figure 4. Over these length scales, features in the concentration profiles are strongly smoothed out by thermal fluctuations relative to ASCMF predictions, and the stratification of long and short chains is diminished.

In addition, under Θ conditions differences between ASCMF and experimental $\Phi(z)$ become pronounced (Figure 4B,D). The differences originate from weaker chain stretching due to poorer brush/solvent compatibility. The chain portions in the sparser outer brush region are particularly sensitive to lowered solvent quality due to their smaller surface densities σ_o (Table 1) and weaker lateral overlap, which allow them to contract more than in the crowded inner brush. This can be directly confirmed from parts E and F of Figure 4 by noting how much the long chains stretch past the short chains. In toluene they stretch $\sim 1.2R_{gz}$ farther than the short chains and thus lead to a distinct contribution of the outer region to the overall shape of the brush. In contrast, in cyclohexane the outer region is unnoticeable due to the weak local chain stretching and the long chains only stretch $\sim 0.6R_{gz}$ past the short chains. Since the theory assumes a priori that the chains are strongly stretched under all solvent conditions, it leads to a distinct outer region in the $\Phi(z)$ profiles for the case of Θ solvents as well as for good

solvents.[9,10] The stretching of the brush could be experimentally enhanced by employing higher molecular weight polymers and surface densities, presumably leading to a more quantitative agreement with ASCMF predictions.

Conclusions

In summary, we have applied neutron reflectivity to examine the structure of bidisperse brushes. Our results furnish direct experimental evidence of a stratified organization in which the length of a polymer dictates the vertical distribution of its segments, a feature useful for the tailoring of polymer modified surfaces. Under both good and Θ solvent conditions the longer chain profiles exhibited a maximum near the brush periphery. The presence of a size-sensitive stratification qualitatively agrees with analytical self-consistent mean field predictions,[9,10] but there are quantitative differences. In particular, the stratification of long and short chains is less pronounced than predicted. Furthermore, while we observe good agreement between ASCMF theory and experiment with regard to the total volume fraction profile (sum of long and short chain profiles) under good solvent conditions, in the presence of a Θ solvent the agreement noticeably worsens. Additional measurements for a variety of compositions and molecular weights should help identify the parameters most useful in determining the degree of stratification and the structure of bidisperse brushes.

Acknowledgment. Financial support from a graduate National Science Foundation Fellowship (R.L.) and the Earl E. Bakken Endowment Funds at the University of Minnesota are gratefully acknowledged.

References and Notes

(1) Halperin, A.; Tirrell, M.; Lodge, T. P. *Adv. Polym. Sci.* **1992,** *100*, 31. Milner, S. T. *Science* **1991**, *251*, 905.
(2) Alexander, S. *J. Phys. (Paris)* **1977**, *38*, 983. de Gennes, P.-G. *Macromolecules* **1980**, *13*, 1069.
(3) Cosgrove, T.; Heath, T. G.; Phipps, J. S.; Richardson, R. M. *Macromolecules* **1991**, *24*, 94.
(4) Auroy, P.; Mir, Y.; Auvray, L. *Phys. Rev. Lett.* **1992**, *69*, 93.
(5) Field, J. B.; Toprakcioglu, C.; Ball, R. C.; Stanley, H. B.; Dai, L.; Barford, W.; Penfold, J.; Smith, G.; Hamilton, W. *Macromolecules* **1992**, *25*, 434.
(6) Karim, A.; Satija, S. K.; Douglas, J. F.; Ankner, J. F.; Fetters, L. J. *Phys. Rev. Lett.* **1994**, *73*, 3407.
(7) Kent, M. S.; Lee, L. T.; Factor, B. J.; Rondelez, F.; Smith, G. S. *J. Chem. Phys.* **1995**, *103*, 2320.
(8) Kent, M. S.; Factor, B. J.; Satija, S. K.; Gallagher, P. D.; Smith, G. S. *Macromolecules* **1996**, *29*, 2843.
(9) Milner, S. T.; Witten, T. A.; Cates, M. E. *Macromolecules* **1989**, *22*, 853.
(10) Birshtein, T. M.; Liatskaya, Y. V.; Zhulina, E. B. *Polymer* **1990**, *31*, 2185.
(11) Dan, N.; Tirrell, M. *Macromolecules* **1993**, *26*, 6467.
(12) Chakrabarti, A.; Toral, R. *Macromolecules* **1990**, *23*, 2016.
(13) Lai, P.-Y.; Zhulina, E. B. *Macromolecules* **1992**, *25*, 5201.
(14) Lauffenburger, D. A.; Linderman, J. J. *Receptors: Models for Binding, Trafficking and Signaling*; Oxford University Press: New York, 1993.
(15) Dhoot, S.; Watanabe, H.; Tirrell, M. *Colloids Surf.* **1994**, *86*, 47.
(16) Kumacheva, E.; Klein, J.; Pincus, P.; Fetters, L. J. *Macromolecules* **1993**, *26*, 6477.
(17) Napper, D. H. *Polymeric Stabilization of Colloidal Dispersions*; Academic Press: New York, 1983.
(18) Klein, J. *Annu. Rev. Mater. Sci.* **1996**, *26*, 581.
(19) Levicky, R. Ph.D. Dissertation. University of Minnesota, 1996.
(20) SLD = $\sum\Phi_i$ SLD$_i$, where Φ_i is the volume fraction of species i and SLD$_i$ is the value for the pure compound.
(21) Russell, T. P. *Mater. Sci. Rep.* **1990**, *5*, 171. Penfold, J.; Thomas, R. K. *J. Phys. C* **1990**, *2*, 1369.
(22) Levicky, R.; Koneripalli, N.; Tirrell, M.; Satija, S. K.; Gallagher, P. D.; Ankner, J. F.; Kulasekere, R.; Kaiser, H. Submitted for publication in *Macromolecules*.
(23) Parratt, L. G. *Phys. Rev.* **1954**, *95*, 359.
(24) Two volume fraction profiles can be uniquely obtained from an SLD profile, but in the interfacial region three components are present: P2VP, PS, and solvent. We assumed a tanh decay of the P2VP profile in order to estimate the volume fraction of PS in the interfacial region.
(25) Noda, I.; Higo, Y.; Ueno, N.; Fujimoto, T. *Macromolecules* **1984**, *17*, 1055.
(26) Strazielle, C.; Benoit, H. *Macromolecules* **1975**, *8*, 203.
(27) Tirrell, M.; Parsonage, E.; Watanabe, H.; Dhoot, S. *Polym. J.* **1991**, *23*, 641.
(28) Milner, S. T.; Witten, T. A.; Cates, M. E. *Macromolecules* **1988**, *21*, 2610. Zhulina, E. B.; Borisov, O. V.; Priamitsyn, V. A. *J. Colloid Interface Sci.* **1990**, *137*, 495.

MA971278N